

Experimental evidence for the use of ultrasound to increase tumor-cell radiosensitivity

Giovanni Borasi¹, Giorgio Russo², Fabrizio Vicari³, Alan Nahum⁴, Maria Carla Gilardi¹

¹IBFM-CNR, Segrate, MI, Italy; ²IBFM-CNR-LATO, Cefalù, PA, Italy; ³LATO, Cefalù, PA, Italy; ⁴The Clatterbridge Cancer Centre, NHS Foundation Trust, Bebington, UK

Correspondence to: Giovanni Borasi. Istituto di Bioimmagini e Fisiologia Biomolecolare del Consiglio Nazionale delle Ricerche, Via Flli Cervi, 93, 20090 Segrate, Milano, Italy. Email: giovanni.borasi@gmail.com.

Abstract: One of the most promising applications of ultrasound (US), and in particular of high intensity focused US (HIFU), exploits its capability to increase the sensitivity of cells and tissues to ionizing radiation. We will discuss the different mechanism hypothesized both for normal and cancerous tissues. To give the reader a more general perspective, we describe in some detail the “classical” mechanism underlying the radiosensitization, independently of the technical methodology adopted. In this context, we will mention the competitive devices, based on electromagnetic waves, which are also able to increase tissue sensitivity and which are already present in the radiotherapy (RT) world. Then we will concentrate on US as the radiation producing the sensitivity increase. Two main aspects will be treated: thermal and non-thermal effects, in particular in association with microbubbles and nanotechnologies.

Keywords: Radiotherapy (RT); ultrasound (US); hyperthermia (HT); radiosensitization; new oncology treatments

Submitted Oct 10, 2014. Accepted for publication Oct 21, 2014.

doi: 10.3978/j.issn.2218-676X.2014.10.05

View this article at: <http://dx.doi.org/10.3978/j.issn.2218-676X.2014.10.05>

Hyperthermia (HT) to improve tissue radiosensitivity

Cell results

The use of heat (HT) to treat cancer is probably one of the oldest cancer therapies known [a description of this technique is reported, for example, in a surgical Egyptian papyrus, in the Indian traditional medicine (Ayurveda) and in the Hippocrates writings]. We can trace back to a 1972 paper from Ben-Hur *et al.* (1), the demonstration of HT as an enhancer of Rx effect on the living material. The experimental premise of this discovery was, however, the single-cell tissue culture technique, introduced by Puck and his associates (2) in 1956. One of the first questions which it was necessary to answer was the dependence of this effect on radiation quality. *Figure 1*, taken from the work Gerner and Leith (3) show the survival curves (SV) of exponentially growing Chinese hamster ovary (CHO) cells exposed in two very different radiation qualities: “sparsely ionizing” (or low-LET) 4 MeV X-rays and “densely

ionizing” (or high LET) Carbon-12 ions. Irradiation was carried out after incubation for 1 h either at 37 °C or at 43 °C. Firstly, comparing the X-ray curves at the two different temperatures, the huge reduction in survival for the same dose is clearly evident. For example, at 5 Gy the survival ratio (called TER, i.e., thermal enhancement ratio) is more than a factor 100. This survival reduction at the higher temperature is accompanied by the nearly total disappearance of the “shoulder” of the curve (on a semilogplot). This suggests that the DNA “repair” processes responsible for this “resistance” to radiation damage are severely impaired by heat. This effect is called “thermal radiosensitization”. In the recent literature there is some discussion about which process is the most effective, double strand break (DSB) repair inhibition of DNA (4) or base damage (5). Another feature evident in the 43 °C X-ray curve is that, even with no radiation, the starting point is considerably lower than for the 37 °C curve. In other words, heat has an intrinsic cell-killing effect.

The administration of heat to living material has a long

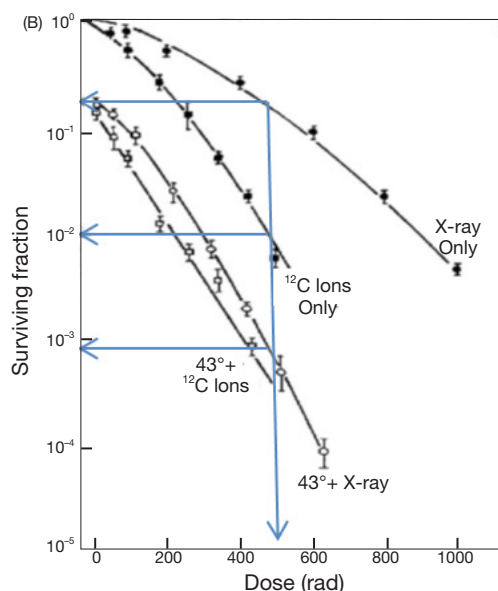


Figure 1 This figure reported the survival fractions on Chinese hamster ovary (CHO) cells of X-ray and ^{12}C ions at the Bragg peak. The curves are obtained without and with hyperthermia (1 hour at 43 °C). The survival of the X-ray curve with hyperthermia is lower than the normal ^{12}C curve. TER value can be very high, with X-rays with hyperthermia becoming even 10 times more effective than ^{12}C ions (without hyperthermia). Reproduce from reference (3).

history, that goes back to Arrhenius theory in 1889 (6). A landmark step in the quantification of this phenomenon was made by Sapareto and Dewey [1984], who found a link between the time and temperature producing the same killing effect on the cells. This result led to the concept of the “thermal dose” as the dose limit at which no living entity (cell or tissue) can survive. This condition is named “ablation”, that means: protein denaturation, cell structure destruction, small vessels coagulation. This thermal dose was expressed in term of cumulative equivalent minutes (CEM) (often referred to 43 °C). Over 43 °C an increase of 1 °C corresponds to a reduction of the exposure time by a factor of two, while under 43 °C a decrease of 1 °C corresponds to an increase of the required time by a factor of four. It’s important to consider that when we apply to clinic HT and radiation, both these phenomena (thermal radiosensitization and heat direct killing) are involved. The loss of the shoulder of the SV curve due to HT clearly remember what happens when irradiation of living material is done in an oxygen rich environment: in this case the oxygen enhancement ratio (OER) play the role of TER. The two phenomena are, obviously linked and both rely on

the quoted cell repair mechanism. As is shown in *Figure 1*, the X-ray TER is much higher that the corresponding value for ^{12}C ions, so that the heated X-ray curve is lower than non-heated ^{12}C ions.

Looking at the survival scale we can see that X-ray with HT, at 500 rad (5 Gy), are about 10 times more effective than ^{12}C ions (without HT). If this result could be integrally translated into patient cure it would change profoundly the future strategy of radiotherapy (RT), and X-ray plus HT may really become the “poor man’s” high LET radiation, as was jokingly reported in the Dewey *et al.* 1977 paper (7). This capability of the Rx plus HT radiation to act like high LET radiation is of the greatest importance dealing with cell in an oxygen deprived environment (or hypoxic), that are quite insensitive to Rx alone, but a good target for high LET radiation and, clearly, also for the Rx plus HT treatment.

To study quantitatively the combination effect, the synergy (*Syn*) concept can be introduced. Mathematically, if SF_a and SF_b are the survival when the radiations a and b are administered independently and SF_{ab} is the survival when bot radiations are administered at the same time, the synergy, Syn_{ab} is defined as:

$$Syn_{ab} = \frac{SF_a \cdot SF_b}{SF_{ab}} \quad [1]$$

This concept is clarified in several papers, in particular in the work of Sapareto *et al.* (8), from which was taken (and redrawn) the following figure (*Figure 2*):

The two curves showing the synergistic effect are calculated following the Eq. [1] and reported in the following figure (*Figure 3*).

In the *Figure 3*, it’s evident the advantage of the midpoint irradiation and the flattening at the higher temperatures of the curve obtained with irradiation three minutes after heath. Both curve peaks about at 43 °C. The authors report that for the synergistic effect obtained with radiation 3 minutes after the heating is conserved even if the interval increases until about 10 minutes. Previous studies by Sapareto *et al.* (9) show that a break occurs in the Arrhenius plot at about 42.5-43.0 °C. This break may indicate that the mechanism of cell inactivation from heat alone is different above and below this temperature transition point, and the data in *Figures 2* and *3* may indicate that there is also a change at 42.5-43.0 °C in the interaction of heat with radiation (it’s known that another break in the Arrhenius plot at 50-52 °C: it would be of the greatest importance to verify if a synergic effect occurs also at these temperatures. These latter could be reached with HIFU, without harm of the patient, for a totally new “deep fast HT”).

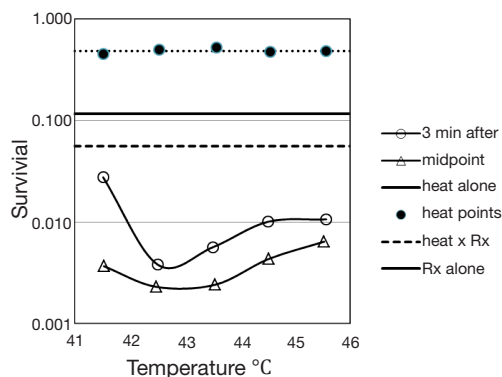


Figure 2 Survival of cells exposed to heat alone or to heat combined with radiation is shown as a function of temperature. Cells were given a heat treatment of 41.5 °C for 92 min, 42.5 °C for 48 min, 43.5 °C for 24 min, 44.5 °C for 12 min or 45.5 °C for 6 min (●). The open circles (○) show survival of cells given the same heat treatments followed 3 min later by a 500 rad dose of X-rays given at 37 °C. The open triangles (△) show the survival of cells given the same heat treatments and irradiated at the treatment temperature (500 rad) such that the midpoint of radiation exposure coincided with the midpoint of heat exposure. Survival for radiation alone, heat alone and the product of the survival of heat and radiation alone (heat × Rx) is also shown. The five points of the heat treatment [41.5 °C for 92 min, 42.5 °C for 48 min, 43.5 °C for 24 min, 44.5 °C for 12 min or 45.5 °C for 6 min] are chosen to give, at different temperature, the same “Thermal dose” and correspond to the same SF (about 0.48). The X-ray is chosen to give a SF of about 0.12. The product of the survivals is then about 0.056. Reproduce from reference (8).

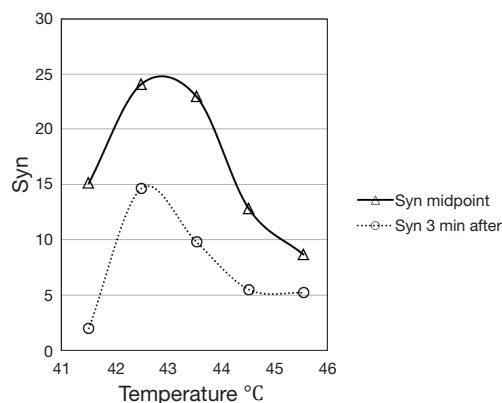


Figure 3 The synergistic effect between radiation and heat [Eq. [1]], obtained following the protocol previously described and reported in *Figure 2*. It's evident the advantage of the midpoint irradiation and the flattening at the higher temperatures of the curve obtained three minutes after.

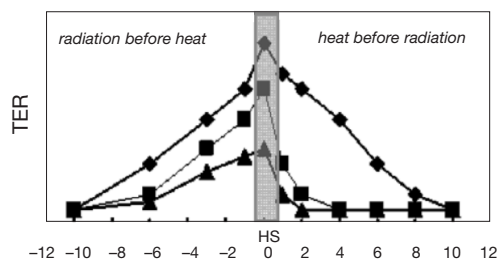


Figure 4 Schematic representation of magnitude of radiosensitization (TER) for mild (triangles) or severe (diamonds) radiation treatment given before (left), simultaneously (grey region) or after heating. Squares represent cell made thermotolerant by a prior heating. Reproduce from reference (11).

While there is a general concordance about the fact that the maximum of the synergistic effect would be if RT and HT are given at the same time (10) (with all the related technical problems), the biological mechanisms invoked are different, as different is the steepness of the curves approaching the maximum. A nice figure from Kampinga (11) may help to understand this point (*Figure 4*).

The starting point is that the activation energies for protein denaturation and heat-induced cell death are within the same range of HT (12). As a result of denaturation, proteins are prone to aggregation and, without the action of chaperones, like heat shock proteins (HSP), these aggregates can have destructive consequences for many macro-molecular structures and their functions. An in deep discussion on this regard can be found in the paper

of Rylander *et al.* (13). So a release of HSP before the heat shock may induce thermotolerance (TT). That explicate the great reduction in the TER in the TT cells (squares in the figure) when heat is given before radiation: with this sequence, a similar mechanism reduce the TER when the radiation treatment is less severe (but not if the radiation level is high!). For low radiation levels, the TER remains higher when radiation is given before heating (as is in the clinical practice today). Whereas the decline in radiosensitization for heat given before radiation is, therefore, modulated by TT, the loss of interaction for radiation before heating, is heat damage independent and solely dependent on the kinetics of repair DNA damage by the cells. In fact if all DNA lesions are repaired before heating, no sensitization occurs.

Looking at the cell cycle, another important reason exist to combine Rx and HT: the S phase that is normally radioresistant, is the most sensitive to HT (7), in contrast cells in G2, M and G1 phases are the most sensitive to ionizing radiations.

Radiofrequency based hyperthermia (HT) devices and radiotherapy (RT)

In a clinical perspective what we said about cells become of practical interest but also new effects came into play. Together surgery and chemotherapy, RT is a one the basic anti-tumor therapies. This latter therapy consists in the irradiation of tumors with high energy radiations (X-ray radiations or particles, like electron or ions). About 50 % of all oncologic patients is treated with this technique (14) and in about 40% of them it gives a substantial contribute to the cure (15). It helps to locally control cancer proliferation, improving patient survival (16), but better overall results are generally obtained by combining RT with other therapeutics. Tumor can be considered as an autonomous organ, with specific hallmarks (17,18) and an highly specialized microenvironment, characterized by a reduced blood flow and a chaotic vasculature with an improved permeabilization, which in turn promote regions of acidosis, hypoxia and ATP energy deprivation. Furthermore, in tumors undergoing RT, adaptive responses, elicited by irradiation itself or by radiation-induced microenvironmental changes, could cause cellular plasticity such that non-stem cancer cells (CSC) acquire CSC properties to become radioresistant (19). Tumor reoxygenation itself changes the redox environment, activating HIF-1 which acts as a powerful radio protective factor for tumors (20). As we quoted before, hypoxic cells are (two or three times) more radioresistant than normoxic ones and their presence and extent correlate with a poor prognosis for different cancer (21). These regions are very sensitive to RT plus RT combination (12,22-24). At the relatives mild temperatures used in the clinical context (<42-43 °C), this effect may not primarily due to thermal death and increased cellular radiosensitization, that we mentioned before in the cellular context, but to the improved tumor blood flow and tumor oxygenation (25,26). Additionally, HT may leads to systemic immune activating effect (27). If no mean exist for a selective heating of tumor, one should try to make the best possible use of a differential effect between health and cancerous tissue. At this regard there is some indication that in tumors some thermal enhancement may be present even when heating follows RT of four or

more hours (23,28). All these experimental results oriented the RT plus HT combined therapy to a quite agreed protocol consisting in administering first RT and then HT, for about 60-90 min at 41.5-43 °C. The effectiveness of the combined HT and RT treatment is relevant in several diseases, like head and neck, esophageal, melanoma, rectal, breast, cervical and soft tissue sarcoma cancers (29,30). Due to the increased blood flow and vessels permeability induced into the tumors, combined treatments may include chemotherapy (31,32) and specialized, heat sensitive, vectors, like liposomes have been developed (for example Caelix[®] or ThermoDox[®], including doxorubicin). As we will discuss later, the same strategy is in use with high intensity focused ultrasound (FUS or HIFU).

The clinical development of HT is tightly linked to the development of a new generation of systems based on radiative antennas, used for superficial and deep heating (33-36), temperature control and treatment planning (37-40). In these systems, a certain degree of warming selectivity is obtained by matching the phases of the antennas only inside the preselected target. The problem of maintaining a uniform temperature even at the interfaces of different tissues is not negligible and is addressed in the more recent literature. It's interesting to note that the MRI technology presently in use for controlling HIFU (proton resonance shift thermometry) was also proposed for hybrid HT-MRI systems (41,42). In the same perspective, the cell killing linear quadratic model was modified to account for hypoxia (43) and HT contribution (44). Deep seated tumors, such as pelvic carcinomas, are generally heated with phased-array systems operating at a frequency between 60 and 140 MHz. Examples of modern 3D steered heating systems are: BSD Sigma eye (45), AMC-8 (46), Alba 4D (47), HYPERCollar (48).

RT plus HT (or HIFU) may have an important role in developing predictive biomarkers and personalized medicine (49).

Effects of low intensity ultrasound (US) on cells

Differently from X-ray, US are mechanical (non electromagnetic) waves travelling into the matter and producing a variety of effects. The use of US as a physical power has been introduced to many fields long ago including industry, chemistry and in medical diagnosis (echography) and therapy (discussed in previous chapter). US in the medical field has been appreciated for its convenience as being an inexpensive and non-invasive method. The number of studies on the possible applications of US is countless (50). US can determine both thermal and non-

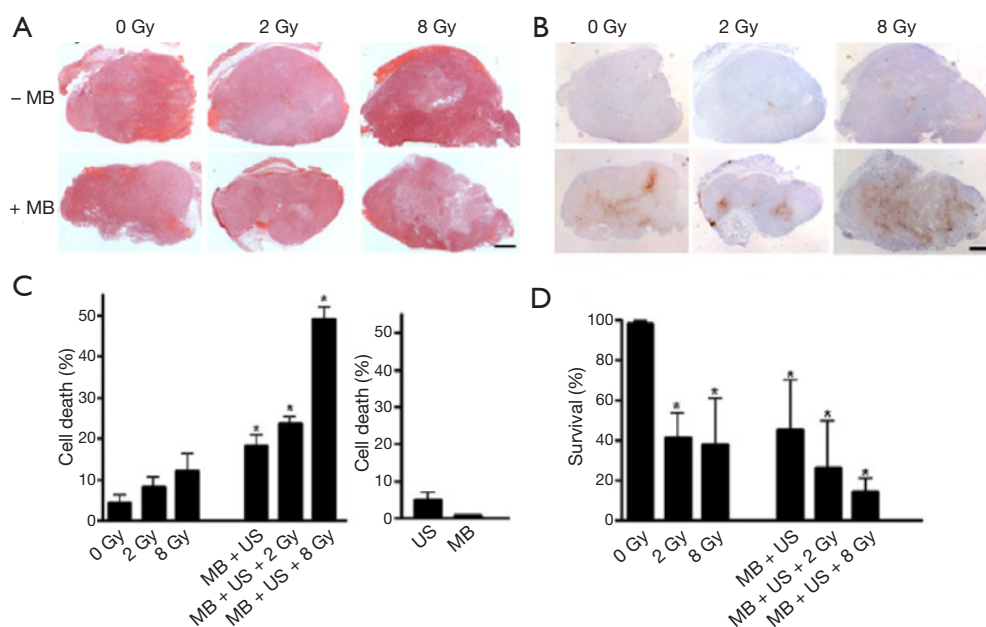


Figure 5 Histopathology, in situ end labeling (ISEL) and clonogenic assays of a PC3 xenograft tumor. (A) H&E staining of whole tumor sections treated with 0, 2 and 8 Gy or with a combination of radiation and ultrasound-stimulated microbubbles (–MB indicates no exposure to ultrasound-stimulated microbubbles; +MB indicates treatment with ultrasound-stimulated microbubbles); (B) sections adjacent to those in were labeled with ISEL to illustrate areas of cell death (scale bars: 1 mm); (C) quantified analyses of ISEL images, indicating an increased level of cell death with the combined treatments. A Mann-Whitney test was used to calculate the P value and * symbols indicate where P value are less than 0.05; (D) clonogenic assay results illustrated a significant decrease in cellular survival of treated tumor cells when compared to the untreated samples. This was greatest in the combined treatments. A Mann-Whitney test was used to calculate the P value and * symbols indicate where P value are less than 0.05. Reproduce from reference (56).

thermal (mechanical) stresses. These latter originate mainly from part of the input energy absorbed by the medium and is reflected as an increase in temperature. Mechanical stresses can either determine or not cavitation. Cavitation stresses can be attributed to the liquid jets produced by collapsing cavities in case of inertial cavitation (51). In the latter case, the potential energy of collapsing bubbles can be converted partly into heat forming high temperature hot spots that reach several thousands of degrees Kelvin at the centre of collapse which, with increased pressure, affect the production of free radicals, the criterion that serves as a test for inertial cavitation. Non-cavitation stresses are caused by “acoustic streaming” (convection) due to the transfer of part of the beam momentum to the liquid and by “microstreaming” and “acoustic pressure” produced by stable oscillating bubbles. It’s common practice to define “low intensity” US when the intensity is lower than 3 W/cm² and, in this case, mainly non-thermal effects are produced, in particular when pulsed US are employed. In the Oncology field, the most important effects

are: Sonodynamic therapy (i.e., the generation of active radicals), enhancement of chemotherapy, gene and apoptosis therapies (52). Low intensity pulsed US has demonstrated a distinct sensitivity for normal and malignant cells (53) able to enhance cancer cell killing induced by X-irradiation (54).

Effects of low intensity ultrasound (US) on tissues

Very impressive results were obtained on xenograft tumors by mixing X-ray, pulsed US and microbubbles by the Czarnota group (55-57). The following figure is taken from the Al-Mahrouki *et al.* paper (Figure 5) and shows histopathology, in situ end labeling (ISEL) and clonogenic assays of a PC3 xenograft tumor.

Preclinical and clinical results using high intensity focused ultrasound (HIFU) devices to enhance the radiotherapy (RT) treatment

A first experiment was executed in China (Peking

University First Department) on the swine model, using both clinical RT (Varian 21EX, operating 6 MV) and HIFU (YDME FEP-BY02) devices, while the centering was done with a GE LOGICQ 5 echography system. This study (58) aimed to perform an *in vivo* investigation evaluating the injury to the pancreas and adjacent tissue of swine resulting with HIFU combined with RT. A total of 12 domestic swine were divided into four groups: control, HIFU only, RT only and HIFU + RT. The injury to the pancreas, adjacent tissue and tissue within the acoustic path of the HIFU beam was assessed based on gross and histologic findings. The pancreas was modeled as a cylinder of 3-4 cm in diameter. The HIFU irradiation was executed with the animal in a supine position and the same position was reproduced on the RT machine where two isocentric, opposing fields (anterior and posterior) of 10 cm² (on the animal skin) were selected. The HIFU (safety) dose was 600 J and the total RT dose was of 13 Gy. For the targeted region of the pancreas, the score of the combined group was higher than that of the HIFU group and the difference was significant. For the acoustic path tissue, there was no significant difference between the control group and the other groups. HIFU combined with RT increased the injury to the targeted pancreas, without increased injury to tissue outside of the targeted region. What is really interesting is that the RT dose was within 12 hours after HT and, in spite of this, some positive effect was detected.

A second experience (Fox Chase Cancer Center, Philadelphia, USA), on mice model, evaluated the efficacy of the enhancement of docetaxel by pulsed focused US (pFUS) in combination with RT for treatment of prostate cancer *in vivo* (59). LNCaP cells were grown in the prostates of male nude mice. When the tumors reached a designated volume by MRI, tumor bearing mice were randomly divided into seven groups (n=5): (I) pFUS alone; (II) RT alone; (III) docetaxel alone; (IV) docetaxel + pFUS; (V) docetaxel + RT; (VI) docetaxel + pFUS + RT; and (VII) control. MR-guided pFUS treatment was performed using a FUS treatment system (InSightec ExAblate 2000) with a 1.5 T GE MR scanner. Animals were treated once with pFUS, docetaxel, RT or their combinations. Docetaxel was given by i.v. injection at 5 mg/kg before pFUS. RT was given 2 Gy after pFUS. Animals were euthanized 4 weeks after treatment. Tumor volumes were measured on MRI at 1 and 4 weeks post-treatment. Results showed that triple combination therapies of docetaxel, pFUS and RT provided the most significant tumor growth

inhibition among all groups, which may have potential for the treatment of prostate cancer due to an improved therapeutic ratio. Quite inexplicably, (I) + (II) combination results were not reported.

A third experiment (People's Hospital, Peking University, China) was done on the human model (60). The purpose of this study was to assess the therapeutic effects and safety of HIFU and low-dose RT for the treatment of rectal carcinoma. A total of 89 cases of rectal carcinoma, including 20 cases of primary rectal carcinoma and 69 cases of recurrent rectal carcinoma after radical rectectomy, were treated with HIFU from July 1998 to December 2000. Of these, 23 patients had follow-up for more than 1 year. There was complete response (CR) in 22.5%, partial response (PR) in 64.0% and no change (NC) in 13.5%. There were no complications, such as skin burn, visceral perforation or hemorrhage, etc. In the 23 cases with follow-up, the 1-year survival rate was 87.0% (20 of 23) and the 2-year survival rate was 80.0% (12 of 15). It was concluded that HIFU plus low dose RT is a new method to treat rectal carcinoma that has remarkable therapeutic effect and is safe, with no significant side effects.

In this context is to mention the very promising effects obtained with nanotechnology applied to HIFU plus RT. A multifunctional organic-inorganic hybrid nanocapsule based on Bi₂S₃-embedded poly (lactic-co-glycolic acid) (PLGA) nanocapsule has been elaborately designed to combine the merits of both polymeric shell structure and Bi₂S₃ nanoparticles (61). Hydrophobic Bi₂S₃ nanoparticles were successfully introduced into the PLGA nanocapsules via a facile and efficient water/oil/water (W/O/W) emulsion strategy. The elastic polymeric PLGA shell provides the excellent capability of US contrast imaging to the Bi₂S₃/PLGA. Meanwhile, the potential of these microcapsules to enhance the HIFU therapy was demonstrated. Importantly, this research provided the first example of both *in vitro* and *in vivo* to demonstrate the radiosensitization effect of Bi₂S₃-embedded PLGA hybrid nanocapsules against prostate cancer under external X-ray irradiation. Thus, the successful integration of the Bi₂S₃ and PLGA nanocapsules provided an alternative strategy for the highly efficient US guided HIFU/RT synergistic therapy. The quantitative results are summarized in the following table (Table 1).

The possibility of producing HT with HIFU devices is actively pursued by the two companies producing HIFU systems with MRI guidance, both for total body systems (62) and prostate (63).

Table 1 Survival assays of PC3 colonies treated with different concentrations (0, 0.5, 1, 2.5 and 5 mg/mL) of Bi₂S₃/PLGA nanocapsules and different radiation doses (0, 3, 6 and 9 Gy)

Bi ₂ S ₃ / PLGA (mg/mL)	Survival fraction of PC3 cells in different radiation doses (%)			
	0 Gy	3 Gy	6 Gy	9 Gy
0	100	64.42	25.33	5.04
0.5	97.82	53.85	16.13	4.72
1	96.30	49.68	12.30	3.11
2.5	97.42	26.70	6.54	1.51
5	95.62	8.28	4.75	0.93

*, P<0.05, i.e., the difference was statistically significant.

Conclusions

As we have tried to show in this paper, the capability of US or HT (whatever produced) to enhance the RT efficacy is thoroughly documented on cells, tissues and the human model. HIFU devices offer, in addition, ablation capability, arguably the best weapon against hypoxic cells. These regions, often present in solid tumors, are less effectively eliminated by low-LET ionizing radiation, and are a major cause of local RT failure and therefore adverse patient outcome (64).

For the maximum synergistic effect (see *Figures 3,4*), we must apply the two treatments HIFU and RT at the same time or with an only short time interval between them (about 10 min maximum). For this, it will be necessary to develop a totally new integrated device, including real-time echography and CT imaging (65). A sealed HIFU probe should be provided with computer-controlled three-dimensional movement around the patient.

A new device with the above capabilities would be able to combine, at the patient couch, HT, ablation, RT and “drug delivery”, as has been discussed elsewhere (66,67). Our hope is that the companies manufacturing these devices will adopt a more general, patient-oriented, point of view.

Acknowledgements

Disclosure: The authors declare no conflict of interest.

References

1. Ben-Hur E, Bronk BV, Elkind MM. Thermally enhanced radiosensitivity of cultured Chinese hamster cells. *Nat New Biol* 1972;238:209-11.

2. Puck TT, Marcus PI, Cieciura SJ. Clonal growth of mammalian cells in vitro; growth characteristics of colonies from single HeLa cells with and without a feeder layer. *J Exp Med* 1956;103:273-83.
3. Gerner EW, Leith JT. Interaction of Hyperthermia with Radiations of Different Linear Energy-Transfer. *Int J Radiat Biol Relat Stud Phys Chem Med* 1977;31:283-8.
4. Iliakis G, Wu WQ, Wang ML. DNA double strand break repair inhibition as a cause of heat radiosensitization: Re-evaluation considering backup pathways of NHEJ. *Int J Hyperthermia* 2008;24:17-29.
5. Kampinga HH, Dikomey E. Hyperthermic radiosensitization: mode of action and clinical relevance. *Int J Radiat Biol* 2001;77:399-408.
6. Arrhenius S. Über die Reaktionsgeschwindigkeit bei der Inversion von Rohrzucker durch Sauren. *Zeitschrift für Physikalische Chemie* 1889;4:226-48.
7. Dewey WC, Hopwood LE, Sapareto SA, et al. Cellular responses to combinations of hyperthermia and radiation. *Radiology* 1977;123:463-74.
8. Sapareto SA, Raaphorst GP, Dewey WC. Cell killing and the sequencing of hyperthermia and radiation. *Int J Radiat Oncol Biol Phys* 1979;5:343-7.
9. Sapareto SA, Hopwood LE, Dewey WC. Combined effects of X irradiation and hyperthermia on CHO cells for various temperatures and orders of application. *Radiat Res* 1978;73:221-33.
10. Loverock P, ter Haar G. Synergism between hyperthermia, ultrasound and gamma irradiation. *Ultrasound Med Biol* 1991;17:607-12.
11. Kampinga HH. Cell biological effects of hyperthermia alone or combined with radiation or drugs: a short introduction to newcomers in the field. *Int J Hyperthermia* 2006;22:191-6.
12. Dewey WC. Arrhenius relationships from the molecule and cell to the clinic. *Int J Hyperthermia* 1994;10:457-83.
13. Rylander MN, Feng Y, Zimmermann K, et al. Measurement and mathematical modeling of thermally induced injury and heat shock protein expression kinetics in normal and cancerous prostate cells. *Int J Hyperthermia* 2010;26:748-64.
14. Delaney G, Jacob S, Featherstone C, et al. The role of radiotherapy in cancer treatment: estimating optimal utilization from a review of evidence-based clinical guidelines. *Cancer* 2005;104:1129-37.
15. Barnett GC, West CM, Dunning AM, et al. Normal tissue reactions to radiotherapy: towards tailoring treatment dose

- by genotype. *Nat Rev Cancer* 2009;9:134-42.
16. Suit HD, Westgate SJ. Impact of improved local control on survival. *Int J Radiat Oncol Biol Phys* 1986;12:453-8.
 17. Hanahan D, Weinberg RA. Hallmarks of cancer: the next generation. *Cell* 2011;144:646-74.
 18. Boss MK, Bristow R, Dewhirst MW. Linking the history of radiation biology to the hallmarks of cancer. *Radiat Res* 2014;181:561-77.
 19. Rycaj K, Tang DG. Cancer stem cells and radioresistance. *Int J Radiat Biol* 2014;90:615-21.
 20. Moeller BJ, Dewhirst MW. HIF-1 and tumour radiosensitivity. *Br J Cancer* 2006;95:1-5.
 21. Brown JM, Wilson WR. Exploiting tumour hypoxia in cancer treatment. *Nat Rev Cancer* 2004;4:437-47.
 22. Dewhirst MW, Viglianti BL, Lora-Michiels M, et al. Basic principles of thermal dosimetry and thermal thresholds for tissue damage from hyperthermia. *Int J Hyperthermia* 2003;19:267-94.
 23. Horsman MR, Overgaard J. Hyperthermia: a potent enhancer of radiotherapy. *Clin Oncol (R Coll Radiol)* 2007;19:418-26.
 24. van der Zee J. Heating the patient: a promising approach? *Ann Oncol* 2002;13:1173-84.
 25. Oleson JR. Eugene Robertson Special Lecture. Hyperthermia from the clinic to the laboratory: a hypothesis. *Int J Hyperthermia* 1995;11:315-22.
 26. Song CW, Park HJ, Lee CK, et al. Implications of increased tumor blood flow and oxygenation caused by mild temperature hyperthermia in tumor treatment. *Int J Hyperthermia* 2005;21:761-7.
 27. Dewhirst MW, Vujaskovic Z, Jones E, et al. Re-setting the biologic rationale for thermal therapy. *Int J Hyperthermia* 2005;21:779-90.
 28. Overgaard J. Simultaneous and sequential hyperthermia and radiation treatment of an experimental tumor and its surrounding normal tissue in vivo. *Int J Radiat Oncol Biol Phys* 1980;6:1507-17.
 29. Palazzi M, Maluta S, Dall'Oglio S, et al. The role of hyperthermia in the battle against cancer. *Tumori* 2010;96:902-10.
 30. Schildkopf P, Ott OJ, Frey B, et al. Biological rationales and clinical applications of temperature controlled hyperthermia--implications for multimodal cancer treatments. *Curr Med Chem* 2010;17:3045-57.
 31. Issels RD. Hyperthermia adds to chemotherapy. *Eur J Cancer* 2008;44:2546-54.
 32. McDaniel JR, Dewhirst MW, Chilkoti A. Actively targeting solid tumours with thermoresponsive drug delivery systems that respond to mild hyperthermia. *Int J Hyperthermia* 2013;29:501-10.
 33. Stauffer PR. Evolving technology for thermal therapy of cancer. *Int J Hyperthermia* 2005;21:731-44.
 34. Johnson JE, Neuman DG, Maccarini PF, et al. Evaluation of a dual-arm Archimedean spiral array for microwave hyperthermia. *Int J Hyperthermia* 2006;22:475-90.
 35. Fatehi D, van der Zee J, van Rhooon GC. Intra-patient comparison between two annular phased array applicators, Sigma-60 and Sigma-Eye: Applied RF powers and intraluminally measured temperatures. *Int J Hyperthermia* 2011;27:214-23.
 36. Paulides MM, Bakker JF, Zwamborn AP, et al. A head and neck hyperthermia applicator: theoretical antenna array design. *Int J Hyperthermia* 2007;23:59-67.
 37. Wust P, Cho CH, Hildebrandt B, et al. Thermal monitoring: invasive, minimal-invasive and non-invasive approaches. *Int J Hyperthermia* 2006;22:255-62.
 38. Kok HP, Crezee J, Franken NA, et al. Quantifying the Combined Effect of Radiation Therapy and Hyperthermia in Terms of Equivalent Dose Distributions. *Int J Radiat Oncol Biol Phys* 2014;88:739-45.
 39. Kok HP, van den Berg CA, Bel A, et al. Fast thermal simulations and temperature optimization for hyperthermia treatment planning, including realistic 3D vessel networks. *Med Phys* 2013;40:103303.
 40. Paulides MM, Stauffer PR, Neufeld E, et al. Simulation techniques in hyperthermia treatment planning. *Int J Hyperthermia* 2013;29:346-57.
 41. Gellermann J, Wlodarczyk W, Feussner A, et al. Methods and potentials of magnetic resonance imaging for monitoring radiofrequency hyperthermia in a hybrid system. *Int J Hyperthermia* 2005;21:497-513.
 42. Stauffer P, Craciunescu O, Maccarini P, et al. Clinical Utility of Magnetic Resonance Thermal Imaging (MRTI) For Realtime Guidance of Deep Hyperthermia. *Proc SPIE* 2009;7181.
 43. Nahum AE, Movsas B, Horwitz EM, et al. Incorporating clinical measurements of hypoxia into tumor local control modeling of prostate cancer: implications for the alpha/beta ratio. *Int J Radiat Oncol Biol Phys* 2003;57:391-401.
 44. Franken NA, Oei AL, Kok HP, et al. Cell survival and radiosensitisation: modulation of the linear and quadratic parameters of the LQ model (Review). *Int J Oncol* 2013;42:1501-15.
 45. Wust P, Beck R, Berger J, et al. Electric field distributions in a phased-array applicator with 12 channels: measurements and numerical simulations. *Med Phys*

- 2000;27:2565-79.
46. Crezee J, Van Haaren PM, Westendorp H, et al. Improving locoregional hyperthermia delivery using the 3-D controlled AMC-8 phased array hyperthermia system: a preclinical study. *Int J Hyperthermia* 2009;25:581-92.
 47. de Greef M, Kok HP, Correia D, et al. Optimization in hyperthermia treatment planning: the impact of tissue perfusion uncertainty. *Med Phys* 2010;37:4540-50.
 48. Paulides MM, Bakker JF, Hofstetter LW, et al. Laboratory prototype for experimental validation of MR-guided radiofrequency head and neck hyperthermia. *Phys Med Biol* 2014;59:2139-54.
 49. Chi JT, Thrall DE, Jiang C, et al. Comparison of genomics and functional imaging from canine sarcomas treated with thermoradiotherapy predicts therapeutic response and identifies combination therapeutics. *Clin Cancer Res* 2011;17:2549-60.
 50. Buldakov MA, Hassan MA, Zhao QL, et al. Influence of changing pulse repetition frequency on chemical and biological effects induced by low-intensity ultrasound in vitro. *Ultrason Sonochem* 2009;16:392-7.
 51. Pitt WG, Husseini GA, Staples BJ. Ultrasonic drug delivery--a general review. *Expert Opin Drug Deliv* 2004;1:37-56.
 52. Yu T, Wang Z, Mason TJ. A review of research into the uses of low level ultrasound in cancer therapy. *Ultrason Sonochem* 2004;11:95-103.
 53. Lejbkowitz F, Salzberg S. Distinct sensitivity of normal and malignant cells to ultrasound in vitro. *Environ Health Perspect* 1997;105 Suppl 6:1575-8.
 54. Buldakov MA, Feril LB Jr, Tachibana K, et al. Low-intensity pulsed ultrasound enhances cell killing induced by X-irradiation. *Ultrason Sonochem* 2014;21:40-2.
 55. Czarnota GJ, Karshafian R, Burns PN, et al. Tumor radiation response enhancement by acoustical stimulation of the vasculature. *Proc Natl Acad Sci U S A* 2012;109:E2033-41.
 56. Al-Mahrouki AA, Iradji S, Tran WT, et al. Cellular characterization of ultrasound-stimulated microbubble radiation enhancement in a prostate cancer xenograft model. *Dis Model Mech* 2014;7:363-72.
 57. Kim HC, Al-Mahrouki A, Gorjizadeh A, et al. Quantitative ultrasound characterization of tumor cell death: ultrasound-stimulated microbubbles for radiation enhancement. *PLoS One* 2014;9:e102343.
 58. Liu CX, Gao XS, Xiong LL, et al. A preclinical in vivo investigation of high-intensity focused ultrasound combined with radiotherapy. *Ultrasound Med Biol* 2011;37:69-77.
 59. Mu Z, Ma CM, Chen X, et al. MR-guided pulsed high intensity focused ultrasound enhancement of docetaxel combined with radiotherapy for prostate cancer treatment. *Phys Med Biol* 2012;57:535-45.
 60. Jun-Qun Z, Guo-Min W, Bo Y, et al. Short-term results of 89 cases of rectal carcinoma treated with high-intensity focused ultrasound and low-dose radiotherapy. *Ultrasound Med Biol* 2004;30:57-60.
 61. Yao MH, Ma M, Chen Y, et al. Multifunctional Bi2S3/PLGA nanocapsule for combined HIFU/radiation therapy. *Biomaterials* 2014;35:8197-205.
 62. Hijnen NM, Heijman E, Kohler MO, et al. Tumour hyperthermia and ablation in rats using a clinical MR-HIFU system equipped with a dedicated small animal set-up. *Int J Hyperthermia* 2012;28:141-55.
 63. Salgaonkar VA, Prakash P, Rieke V, et al. Model-based feasibility assessment and evaluation of prostate hyperthermia with a commercial MR-guided endorectal HIFU ablation array. *Med Phys* 2014;41:033301.
 64. Dewhirst MW, Cao Y, Moeller B. Cycling hypoxia and free radicals regulate angiogenesis and radiotherapy response. *Nat Rev Cancer* 2008;8:425-37.
 65. Weiss N, Goldberg SN, Sosna J, et al. Temperature-density hysteresis in X-ray CT during HIFU thermal ablation: heating and cooling phantom study. *Int J Hyperthermia* 2014;30:27-35.
 66. Borasi G, Russo G, Alongi F, et al. High-intensity focused ultrasound plus concomitant radiotherapy: a new weapon in oncology? *J Ther Ultrasound* 2013;1:6.
 67. Borasi G, Melzer A, Russo G, et al. Cancer therapy combining high-intensity focused ultrasound and megavoltage radiation. *Int J Radiat Oncol Biol Phys* 2014;89:926-7.

Cite this article as: Borasi G, Russo G, Vicari F, Nahum A, Gilardi MC. Experimental evidence for the use of ultrasound to increase tumor-cell radiosensitivity. *Transl Cancer Res* 2014;3(5):512-520. doi: 10.3978/j.issn.2218-676X.2014.10.05